To be submitted to ApJ Letters

Particle acceleration in stressed coronal magnetic fields

R. Turkmani[1], L. Vlahos[2], K. Galsgaard[3], P. J. Cargill[1] and H. Isliker[2]

ABSTRACT

This letter presents an analysis of particle acceleration in a model of the complex magnetic field environment in the flaring solar corona. A slender flux tube, initially in hydrodynamic equilibrium, is stressed by random photospheric motions. A 3-D MHD code is used to follow the stochastic development of transient current sheets. These processes generate a highly fragmented electric field, through which particles are tracked using a relativistic test particle code. It is shown that both ions and electrons are accelerated readily to relativistic energies in times of order 10^{-2} s for electrons and 10^{-1} for protons forming power law distributions in energy.

Subject headings: Particle acceleration –solar flares- MHD

1. Introduction

Understanding how particles are accelerated in solar flares is a major scientific challenge due to both the large number of accelerated particles ($\sim 10^{38}$ electrons/sec) and the impulsive nature which implies high efficiency for the acceleration mechanism(s).

Recent observations from the Ramaty High Energy Solar Spectroscopic Imager (RHESSI) spacecraft have demonstrated unambiguously that between 10% and 50% of energy release in solar flares ends up in high energy electrons. To this must be added an unknown, but probably significant, level of energization of protons and other ions (e.g. Miller et al. 1997). RHESSI results have also demonstrated that photon spectra have a power-law energy spectrum extending over a few decades consisting of either a single or double power law, combined

[1]Space and Atmospheric Physics group, Imperial College

[2]Department of Physics, University of Thessaloniki, 54124 Thessaloniki, Greece

[3]Niels Bohr Institute for Astronomy Physics and Geophysics, Copenhagen, Denmark

in many cases with a thermal part. One conclusion is that the scale-less power-law spectra are more consistent with particle acceleration at multiple small sites rather than at a single large one (e.g. Lin et al 2003).

The major difficulty in accounting for these observations lies in the fact that fast energy release and particle acceleration occur most effectively on small spatial and temporal scales (sub-km and sub-sec), perhaps in the vicinity of current sheets or shocks, and are best described by a full kinetic description of the plasma. On the other hand observations indicate that a flare encompasses vast regions of the corona (many thousands of km), is probably determined by the response of the coronal field to motions in the photosphere, and will be governed by a magnetohydrodynamic (MHD) description. Developing a flare model that addresses both aspects is stymied by the disparate timescales associated with the two regimes.

Many articles have addressed the problem of particle acceleration in flares from the viewpoint of a single reconnection site, shock or a volume filled with MHD waves (see Miller et al. (1997) and Miller (1998) for a discussion). All such models are very loosely connected to the magnetic energy release process(es). It is likely that direct electric fields, MHD turbulence and shocks are all present in the vicinity of current sheets during magnetic reconnection, or during the initial phase of an expanding magnetic structure (CME), but very little is known about how these processes can energize large numbers of electrons and ions during the impulsive phase (lasting only several seconds).

It thus seems clear that understanding flare particle acceleration may require a change in our perception of the coronal magnetic topology in which energy is released. The formation of many dissipation regions which operate as acceleration sites is an interesting alternative scenario to a single monolithic site of energy release and particle acceleration (Masuda et al. 1994). In such a fragmented energy release processes, particles can interact with multiple acceleration sites (e.g. Anastasiadis, Vlahos & Georgoulis 1997; Vlahos, Isliker & Lepreti 2004; Anastasiadis et al. 2004), and in principle the acceleration at one site can influence the acceleration properties of the others. Recent work along these lines has considered particle acceleration from a viewpoint that tracks ‘test particles’ in a statistically distributed electric field resulting from many small reconnection sites using a Cellular Automata (CA) model (e.g. Vlahos, Isliker & Lepreti 2004; Anastasiadis et al. 2004), or fully-developed MHD turbulence (Dmitruk et al 2003; Arzner & Vlahos. 2004). However, to address the acceleration problem fully, particle acceleration needs to be considered in the context of a realistic coronal magnetic field model. That is the purpose of this paper. We use a 3-D MHD model to determine the coronal field structure as it responds to photospheric motions, and calculate the evolution of charged particles in the electric fields generated by the stressed magnetic fields.

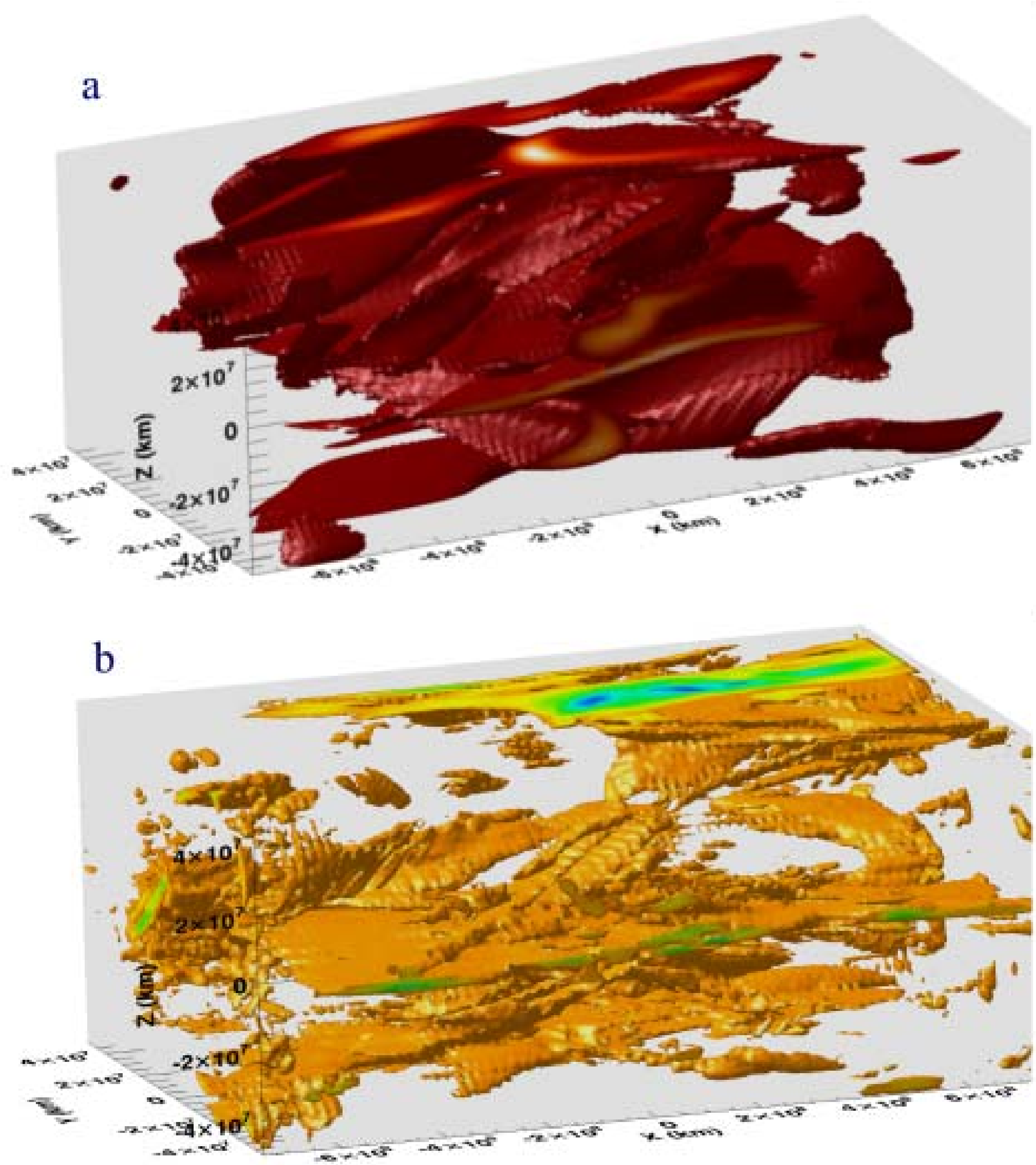

Fig. 1.— Snapshots of the **a** inductive electric field and **b** resistive electric field configurations within the coronal volume, as calculated from the global MHD model. The details of the model are described in the text.

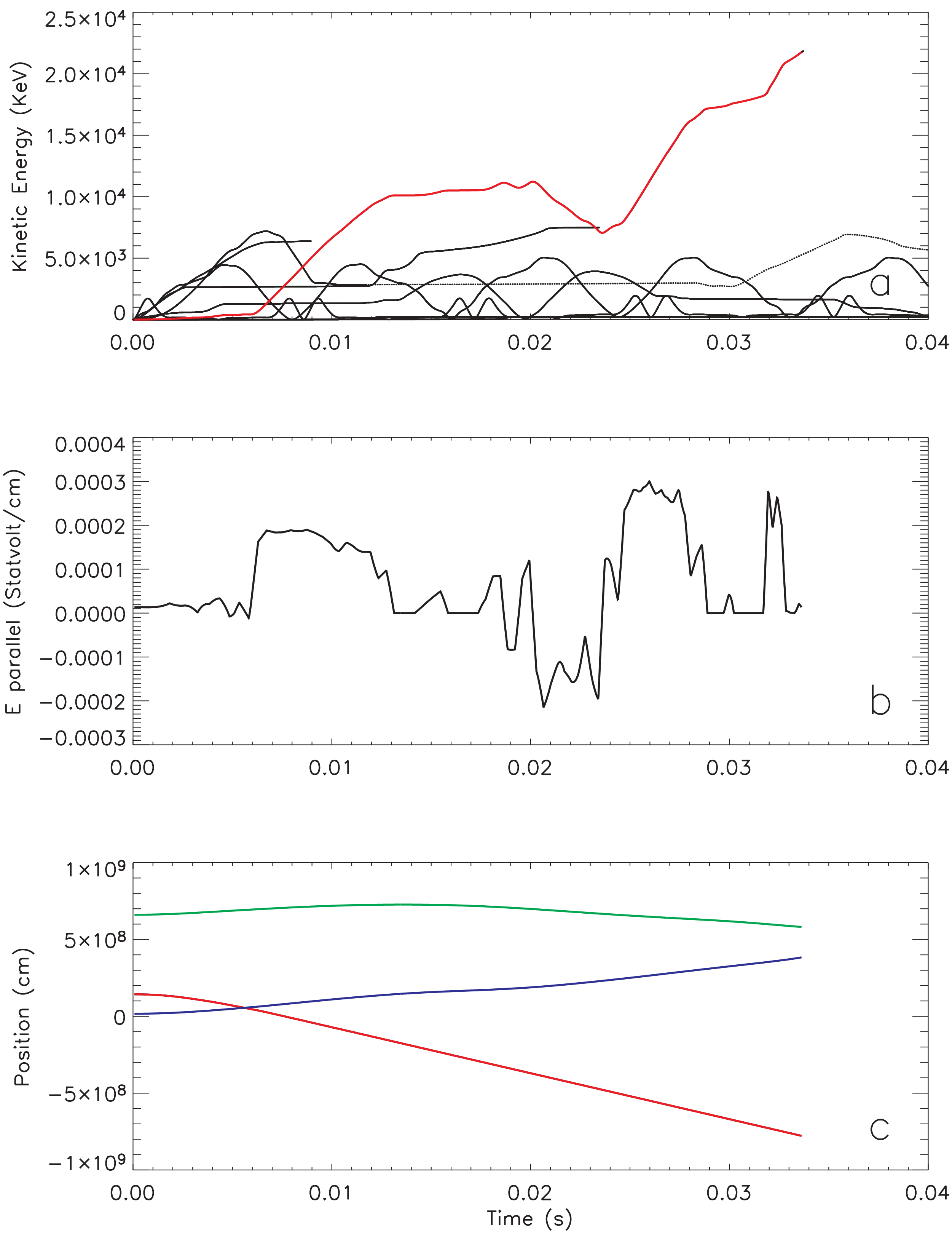

Fig. 2.— **a** The Energy gain versus time for a randomly chosen sample of 10 electrons. **b** The parallel electric field experienced by one electron, shown with the red colour in panel a. **c** The position of the particle given by the x, y and z positions in red green and blue colours respectively. The y and z positions are multiplied with a factor of ten.

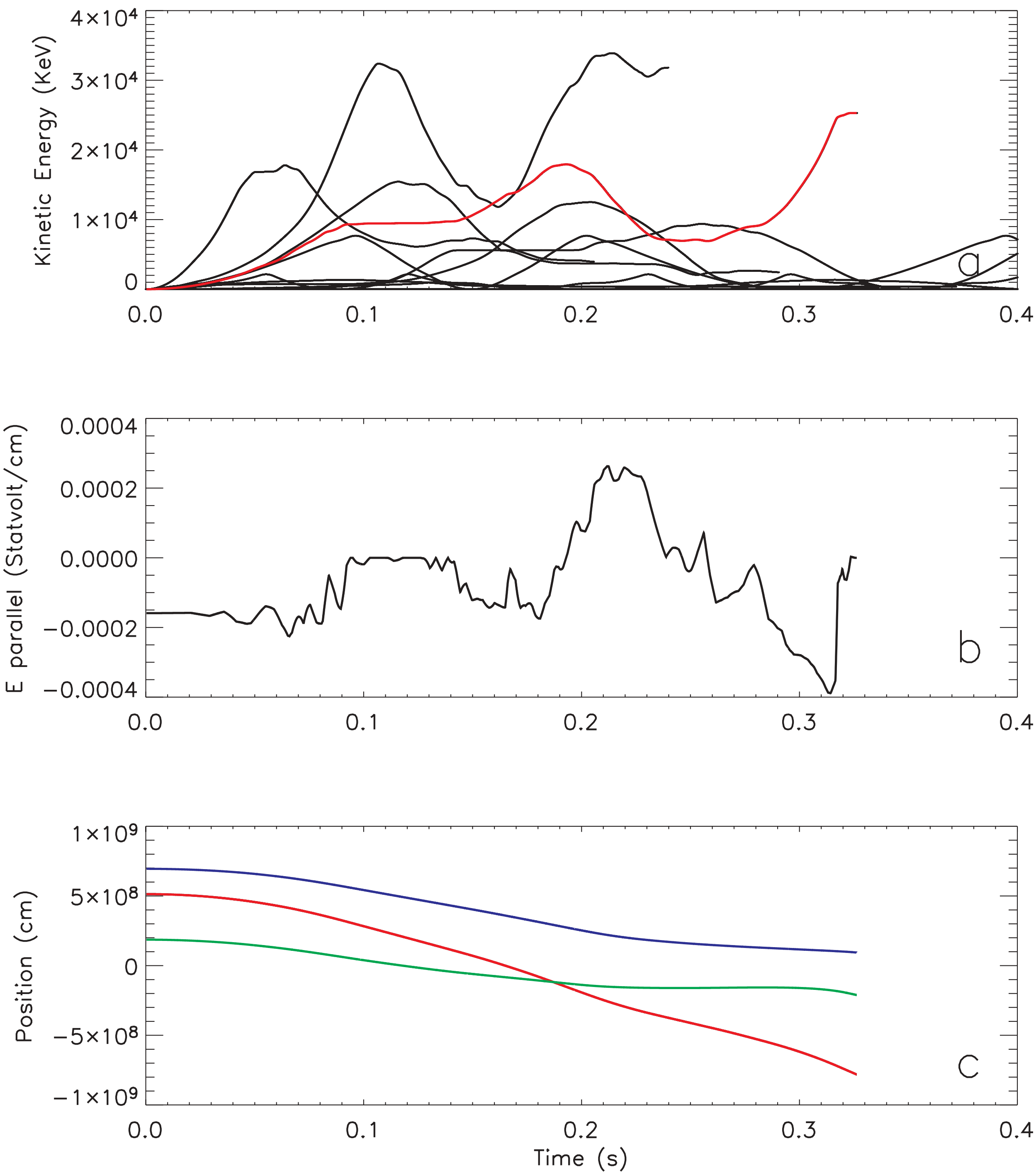

Fig. 3.— **a** The Energy gain versus time for a randomly chosen sample of 10 protons. **b** The parallel electric field experienced by one proton, shown with the red colour in panel a. **c** The position of the particle given by the x, y and z positions in red green and blue colours respectively. The y and z positions are multiplied with a factor of ten.

2. Model Description

The coronal field model used in this article is based on the work of Galsgaard & Nordlund (1996) and Galsgaard (2002) who performed a series of 3-D MHD experiments demonstrating how small-scale coronal structure (such as current sheets) arise from a sequence of simple photospheric boundary motions. The coronal field is assumed to be anchored in the photosphere at both ends, and is 'straightened out': i.e. large-scale magnetic field curvature is ignored. The initial magnetic field is uniform everywhere, while the density changes by a factor of a thousand between photosphere and corona. The atmosphere is initially in hydrostatic equilibrium. Photospheric motions are then imposed at the boundaries using a simple sinusoidal incompressible shear pattern that is randomly changed in time. These boundaries are impenetrable and infinitely conducting so that the imposed boundary motions advect the magnetic footpoints with it and impose stress on the entire system.

The time dependent evolution is followed by numerically solving the 3-D non-ideal MHD equations in Cartesian geometry (Nordlund & Galsgaard 1997) including heat conduction and optically thin radiation. After a few driving periods the magnetic field develops a topology which is highly structured, with strong current concentrations being scattered around the simulation box. More details about the specific numerical experiment are given in Galsgaard (2002), while a discussion of the current sheet formation and distribution is given in Galsgaard & Nordlund (1996).

To study particle acceleration, we chose a snapshot of the coronal magnetic and electric fields and ran test particles through them by solving numerically the relativistic equations of motion. The particle algorithm uses an adaptive time-step, and also requires values of both the magnetic and electric fields at arbitrary positions. These are determined using simple linear interpolation from the MHD solution. The electric field is fully three-dimensional and arises from two distinct sources:

$$\vec{E} = -\vec{V} \times \vec{B} + \eta^* \vec{J} \tag{1}$$

where the first term is the inductive field, and the second is the resistive field which arises due to a finite resistivity, and **V** is the plasma velocity given by the MHD equations. The MHD code utilizes a hyper-resistivity η^* to localize diffusion only to regions where it is required in order to limit steepening of non-linearities (for details see Nordlund & Galsgaard 1997). Figures 1a and 1b show a snapshot of the coronal resistive and inductive fields respectively for a simulation with dimensions 2×10^8 cm in the transverse (y and z) directions and 1.5×10^9 cm along the loop axis (x direction). The highly fragmented structure of both field components is clear and these are associated with magnetic field turbulence with a magnitude of 5 - 10% of the ambient field.

One would expect the first term in (1) to be important outside current sheets, where it will lead to predominately (but not solely) $\vec{E} \times \vec{B}$ drifts, and the second in the vicinity of reconnection sites, where it will lead to acceleration parallel to the ambient magnetic field (see also Dmitruk et al 2003). We focus predominately on cases using the resistive field only, since that is where one expects the predominant energy gain to come from. However, we compare these results to models including both electric field components.

We adopt the following initial physical parameters for the MHD model. The coronal β is small and the magnetic field is taken as 100 G in the axial (z) direction. The anomalous resistivity $\eta^\star$ is either zero or takes on values between 10^{-1} s to 10^{-3} s. These parameters then determine the strength and orientation of the electric field from Maxwell's equations and Ohm's law. We use only the coronal part of the MHD model. Particles that leave the coronal region are considered lost from our system. Both electrons and protons are tracked. We inject the particles starting from a Maxwellian distribution with a temperature of $\sim 1.2^6$ K (The black curve in Fig. 4a). The initial positions of the particles are random, as is their pitch-angle.

3. Results

Fig. 2 shows the properties of 10 arbitrarily chosen electrons. The upper panel shows the energy of the particles versus time, the middle one the parallel electric field experienced by the particle shown in red in panel a, and the lower one the position of this particle. Fig. 3 shows the same parameters as Fig. 2 but for 10 arbitrarily chosen protons. Some of the particles gain a little energy, some gain then lose energy, while a few reach high energies. The timescale for energy gain is significantly less than one second for electrons which get accelerated to tens of Mev within few 10^{-2} seconds. Protons reach roughly the same energy within few 10^{-1} seconds, and both timescales are much shorter than any MHD timescale.

As they undergo acceleration, the particles move through a large portion of the simulation box, and so experience acceleration at a number of current sheets. Some particles exit the box quickly while others remain trapped inside for a longer time. Because of the nature of the photospheric driver, the axial current (and hence $E_\parallel$) can take on either positive or negative values, depending on the nature of the shear in the coronal field. As the particles interact with a current sheet, the reconnection of the field there means that they can move through the simulation, hence sampling flux systems with different photospheric connectivity. Note also that the parallel electric field is two to three orders of magnitude in excess of the Dreicer field.

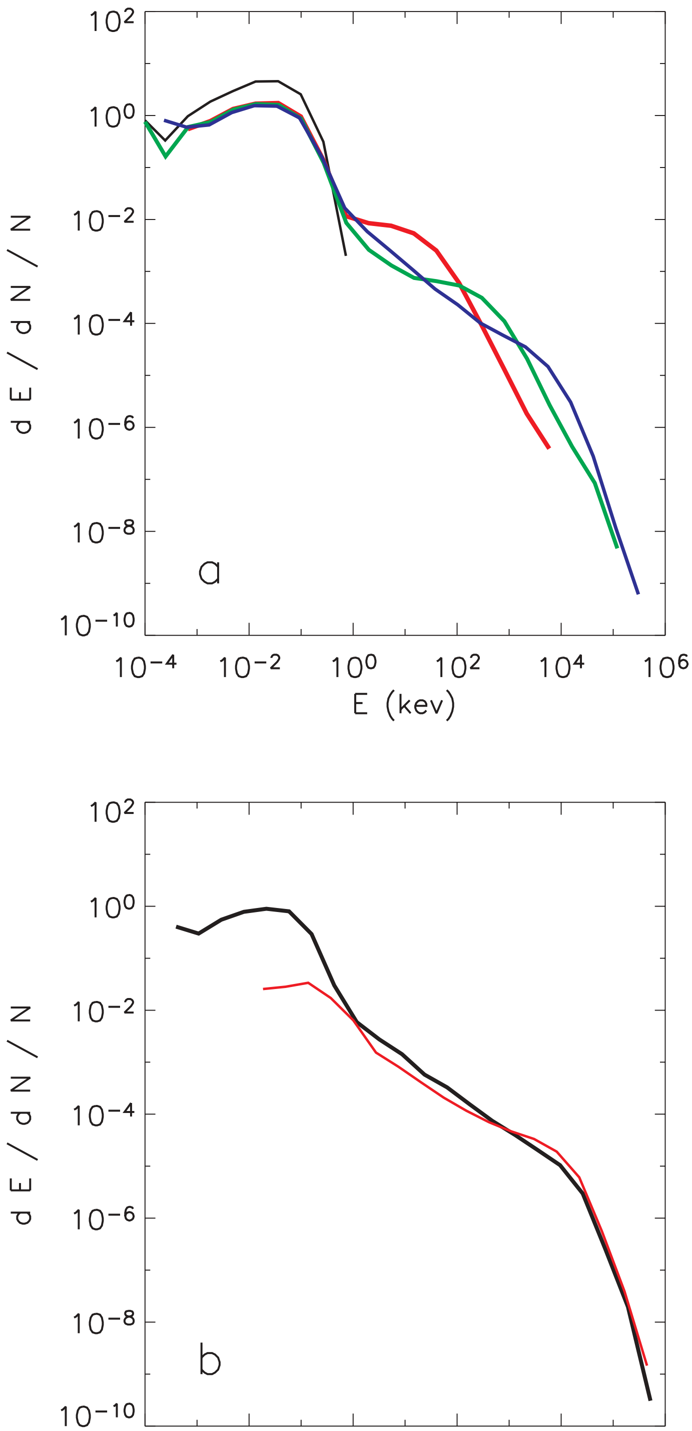

Fig. 4.— The distribution function obtained by running 40,000 electrons in a coronal volume with $L = 1.5 \times 10^9$ cm. **a** The time evolution of the distribution functions taken at $t = 0$ (black), $t_1 = 0.0125$ s (red), $t_2 = 0.025$ s (green) and $t_3 = 0.05$ s (blue). **b** The final distribution function at $t = 0.1$ from the above model considering only the resistive component of the electric field (in black) compared to that of a similar model that consider both the resistive and the inductive components on the electric field (in red).

Particles tend to travel along the field lines if the inductive field is not included. If it is included, the electrons stay close to the field lines while protons tend to travel initially away from the field lines then bend and join the trajectory of a field line. This is similar to the familiar "'ion pick-up"' phenomenon. This is due to the fact that for a proton and an electron with the same initial energy, electrons have a higher velocity which makes contribution from the drift velocity negligible compared to their initial one.

Fig. 4a shows the time evolution of the distribution functions obtained from running 40,000 electrons inside box for a time long enough to allow all free particles to leave the box (0.1 s). The first black curve shows the initial distribution at $t = 0$, whereas the red, green and blue curves show the distribution function at $t_1 = 0.0125$ s, $t_2 = 0.025$ s and $t_3 = 0.05$ s respectively. The final distribution function is shown in black in Fig 4b and is obtained by considering all the particles including those that left the box before the end of the run. Fig. 4a shows that while a certain population of the particles maintain their initial Maxwellian distribution below 1 keV, a tail develops gradually towards the MeV region ending with a cut-off at high energies. In Fig. 4b the final distribution function shows a pronounced power law component between 1 keV and 10 MeV, whereas the distribution after the cut-off extends towards 0.5 GeV.

The red curve in Fig. 4b shows the distribution function resulting from a run that uses both the resistive and inductive electric field components. It shows that the inductive field plays a very small role in the overall acceleration. This is mainly because the parallel component of this field must be zero, and the energy gain in the perpendicular direction is very small compared to that from the parallel resistive field component. However, this perpendicular contribution does show an effect in the region below 1 kev. Particles that remain within this range are mainly those injected in regions where the parallel resistive field is zero. They therefore maintain their thermal distribution but gain some energy when the inductive field is included.

We have examined the scaling of the results with the length of the box. The maximum energy scales up with length of the domain. A temporal scaling also arises here as particles needs more time to travel through a longer domain.

4. Discussion and conclusions

In this article we study for the first time the acceleration of electrons and ions inside a coronal magnetic flux tube stressed by the random motions of the photosphere using a 3-D MHD code. The stochastic development of current sheets which are associated with a distribution of strong electric fields inside the stressed magnetic topology provide the electromagnetic environment in which particles are accelerated. Using a relativistic test particle code, we follow the evolution of an ensemble of electrons and ions. Our main finding is that the electrons and ions are accelerated fast and efficiently along the entire length of the magnetic structure. In relatively short times particles reach relativistic energies and form power law distributions in energy. We also found that the inductive electric field plays very little role in accelerating particles.

We conclude that the stochastic formation of current sheets in complex and stressed by the photosphere magnetic topologies can provide an alternative to the existing models for solar flares.

This work was funded by the European Commission under research training network HPRN-CT-2001-00310. KG acknowledges funding by PPARC in the form of an Advanced Fellowship and Carlsbergfondet in the form of a Scholarship over various periods of the project. PC acknowledges the support of a PPARC senior fellowship.

REFERENCES

Anastasiadis, A., Vlahos, L. & Georgoulis, M. K., 1997, ApJ, 428, 819

Anastasiadis, A., Gontikakis, C., Vilmer, N. & Vlahos, L., 2004, A&A, 422, 323.

Arzner, K. & Vlahos, L., 2004, ApJ, 605, L69

Dmitruk, P., Matthaeus, W. H., Seenu, N. & Brown, M. R., 2003, ApJ, 597, L81

Galsgaard, K., 2002, SOLMAG 2002. Proceedings of the Magnetic Coupling of the Solar Atmosphere Euroconference and IAU Colloquium 188, ESA SP-505.

Galsgaard, K., & Nordlund, A. 1996 J.G.R., 101, 13445

Lin, R. P. et al, 2003, ApJ, 595, L69.

Masuda, S., Kosugi, T., Hara, H., Tsuneta, S. & Ogawara, Y., 1994, Nature, 371, 595.

Miller et al., 1997, JGR, 102, 14631

Miller, J. A., 1998, SSRv, 86, 79

Nordlund, A. & Galsgaard, K., 1997, A 3D MHD Code for Parallel Computers. Technical Report, Astronomical Observatory, Copenhagen University.

Vlahos, L., Isliker, H., & Lepreti, F., 2004, ApJ, 608, 540.
